

## A RECENT EXPERIMENT WITH HYPERBALL\*

Y. MIURA<sup>a</sup>, S. AJIMURA<sup>b</sup>, Y. FUJII<sup>a</sup>, T. FUKUDA<sup>c</sup>, O. HASHIMOTO<sup>a</sup>  
 H. HOTCHI<sup>c</sup>, K. IMAI<sup>d</sup>, W. IMOTO<sup>c</sup>, Y. KAKIGUCHI<sup>e</sup>, S. KAMEOKA<sup>a</sup>  
 A. KRUTENKOVA<sup>f</sup>, T. MARUTA<sup>e</sup>, A. MATSUMURA<sup>a</sup>, K. MIWA<sup>d</sup>  
 T. MIYOSHI<sup>a</sup>, K. MIZUNUMA<sup>a</sup>, S.N. NAKAMURA<sup>a</sup>, T. NAGAE<sup>e</sup>  
 H. NOMURA<sup>a</sup>, H. NOUMI<sup>e</sup>, Y. OKAYASU<sup>a</sup>, T. OTAKI<sup>c</sup>, H. OUTA<sup>e</sup>  
 P.K. SAHA<sup>c</sup>, T. SAITOH<sup>g</sup>, Y. SATO<sup>e</sup>, M. SEKIMOTO<sup>e</sup>, T. TAKAHASHI<sup>a</sup>  
 H. TAMURA<sup>a</sup>, K. TANIDA<sup>h</sup>, A. TOYODA<sup>e</sup>, M. UKAI<sup>a</sup>  
 AND H. YAMAUCHI<sup>a</sup>

<sup>a</sup>Department of Physics Tohoku University, Sendai 980-8578, Japan

<sup>b</sup>Department of Physics Osaka University, Toyonaka 560-0043, Japan

<sup>c</sup>Osaka Electro-Communication University, Neyagawa 572-8530, Japan

<sup>d</sup>Department of Physics Kyoto University, Kyoto 606-8502, Japan

<sup>e</sup>Institute of Particle and Nuclear Studies, KEK, Tsukuba 305-0801, Japan

<sup>f</sup>Institute of Theoretical and Experimental Physics, Moscow 117218, Russia

<sup>g</sup>GSI, Darmstadt D-64291, Germany

<sup>h</sup>RIKEN, Wako 351-0198, Japan

(KEK-PS E518 Collaboration)

(Received February 10, 2004)

Using a germanium detector array, Hyperball, we have measured  $\gamma$  rays from several  $\Lambda$  hypernuclei. In the previous experiments, spin-dependence of  $\Lambda N$  effective interaction was investigated. In the latest experiment, we have studied  ${}_{\Lambda}^{11}\text{B}$  in which six  $\gamma$  transitions have been observed. The result of this experiment suggests that the level structure is quite different from a theoretical prediction based on the  $\Lambda N$  spin-dependent effective interaction parameters determined in the previous experiments.

PACS numbers: 21.80.+a, 21.10.-k, 23.20.-g, 27.20.+n

## 1. Physics motivation

Detailed level structure of hypernuclei enables us to investigate several interesting subjects, such as  $YN$  interactions, hypernuclear shrinking effect, and nuclear medium effect of baryons.

---

\* Presented at the XXVIII Mazurian Lakes School of Physics, Krzyże, Poland, August 31–September 7, 2003.

In recent years, we have developed  $\gamma$  spectroscopy of hypernuclei. By using a large germanium (Ge) detector array, Hyperball, the energy resolution of hypernuclear spectroscopy has been improved from 1–2 MeV to a few keV, and a great progress has been made in studying structure of hypernuclei.

The structure of hypernuclei can be understood by combining a  $\Lambda$  and the other part called “core”. If  $j_{\text{core}} \neq 0$ , one state of the core nucleus splits into two states of the hypernucleus according to the spin direction of a  $\Lambda$  as shown in Fig. 1. Since the energy spacing between these two states is typically of the order of 100 keV, it is necessary for us to use Ge detectors to observe such a fine structure. Such spin doublets are often called “hypernuclear fine structure”.

From precise measurements of  $\gamma$  rays from hypernuclei, the following three subjects can be studied.

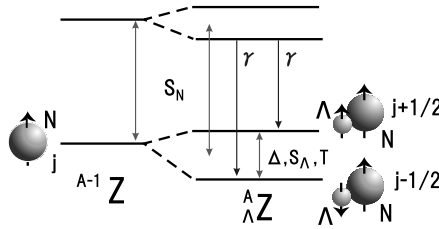


Fig. 1. Hypernuclear fine structure. By observing  $\gamma$  rays from hypernuclei, spin-dependent forces of  $\Lambda N$  interaction can be investigated. See text for details.

### 1.1. $\Lambda N$ effective interaction

By observing  $\gamma$  rays from  $p$ -shell hypernuclei, spin dependence of the  $\Lambda N$  interaction can be investigated. Theoretical estimations which are based on  $\Lambda N$  potential models and available experimental data such as level structure and  $\Lambda$  binding energies of several hypernuclei have been performed to determine  $p_N s_\Lambda$  two-body effective interactions [1,2]. The two-body  $\Lambda N$  effective interaction can be expressed in terms of five radial integrals associated with each term in

$$V_{\Lambda N}(r) = V_0(r) + V_\sigma(r) \mathbf{s}_N \cdot \mathbf{s}_\Lambda + V_A(r) \mathbf{l}_{N\Lambda} \cdot \mathbf{s}_\Lambda + V_N(r) \mathbf{l}_{N\Lambda} \cdot \mathbf{s}_N + V_T(r) \mathbf{S}_{12}, \quad (1)$$

where  $\mathbf{l}_{N\Lambda}$  is the relative orbital angular momentum and

$$\mathbf{S}_{12} = 3(\mathbf{s}_N \cdot \hat{\mathbf{r}})(\mathbf{s}_\Lambda \cdot \hat{\mathbf{r}}) - \mathbf{s}_N \cdot \mathbf{s}_\Lambda$$

with  $r = |\mathbf{r}_N - \mathbf{r}_\Lambda|$ . These five integrals denoted by  $\overline{V}$ ,  $\Delta$ ,  $S_\Lambda$ ,  $S_N$ , and  $T$  are taken to be constant throughout the shell. To obtain explicit expressions for the radial forms appearing in Eq. (1), several versions of Nijmegen models are used as the  $\Lambda N$  potential.

The average central interaction ( $\bar{V}$ ) is determined to reproduce the measured  $\Lambda$  binding energies ( $B_\Lambda$ ) for several  $p$ -shell hypernuclei. The other four parameters express spin-dependent forces. The spin-spin force ( $\Delta$ ), the  $\Lambda$ -spin-induced spin-orbit force ( $S_\Lambda$ ), and the tensor force ( $T$ ) are obtained from hypernuclear fine structure. On the other hand, the nucleon-spin-induced spin-orbit force ( $S_N$ ) causes the difference of nucleon excitation energy between a hypernucleus and its core nucleus. Fig. 1 shows typical low-lying levels of a hypernucleus. Using the shell model calculations, level energies of hypernuclei are described with these parameters and compared with their experimental data to improve the parameters.

The basic philosophy behind this phenomenological approach was proposed by Gal, Soper, and Dalitz [1, 2]. The calculations presented in [1, 2] were improved by Millener [3]. In this calculation, the shell model with  $\{s^4 p^A s_\Lambda\}$  and  $\{s^4 p^A s_\Lambda p_\Lambda\}$  configurations were used, and the effect of three-body  $\Lambda NN$  interaction was also parameterized.

### 1.2. Impurity effect

Inside a nucleus, a  $\Lambda$  in the  $0s$  orbit attracts nucleons around it and causes its shrinkage. This effect is called “glue-like role” of  $\Lambda$  in the nucleus and experimentally confirmed in the case of  ${}^7_\Lambda\text{Li}$  by the KEK-PS E419 experiment. By comparing  $B(E2)$  of  ${}^7_\Lambda\text{Li}$  ( $5/2^+ \rightarrow 1/2^+$ ) with that of the core transition  ${}^6\text{Li}$  ( $3^+ \rightarrow 1^+$ ), it was found that the size of  ${}^7_\Lambda\text{Li}$  is  $19 \pm 4\%$  smaller than that of  ${}^6\text{Li}$  [4]. Such a nuclear shrinking effect is a general property of light hypernuclei, which was pointed out by Motoba *et al.* [5] for the first time and precisely calculated by Hiyama *et al.* [6]

The measurement of  $B(E2)$  was carried out by Doppler shift attenuation method (DSAM). If  $\gamma$  ray emission is fast enough after the production of the hypernucleus, the width of the observed  $\gamma$  ray peak is broadened by Doppler effect. The lifetime of the excited state is obtained from the observed peak shape compared with that from a Monte Carlo simulation. This method can be used when the lifetime of the excited state is comparable with the stopping time of the hypernucleus.

### 1.3. Medium effect of baryons

The properties of baryons in a nucleus may change due to the medium effect, namely, it is expected that the mass of baryons is affected by partial restoration of chiral symmetry. Since a  $\Lambda$  is free from Pauli blocking effect, it can probe the inside of the nucleus. Therefore, the medium effect of baryons can be measured by comparing the  $g$ -factor of a  $\Lambda$  in the nucleus with that in the free space. Because of its short lifetime, it is difficult to measure  $g$ -factors of hypernuclei directly. However, they can be measured from the

B(M1)'s of  $\Lambda$ -spin-flip M1 transitions. If we assume a weak coupling between a  $\Lambda$  and the core nucleus, the B(M1) can be expressed as

$$\begin{aligned} B(M1) &\propto |\langle \phi_f | \mu^z | \phi_i \rangle|^2 \\ &\propto |\langle \phi_A^\dagger \phi_{\text{core}} | g_{\text{core}} \mathbf{j}_{\text{core}}^z + g_\Lambda \mathbf{j}_\Lambda^z | \phi_A^\dagger \phi_{\text{core}} \rangle|^2 \\ &\propto (g_\Lambda - g_{\text{core}})^2. \end{aligned} \quad (2)$$

This equation shows that the  $g$ -factor of a  $\Lambda$  in the nucleus ( $g_\Lambda$ ) can be derived by measuring the B(M1) of the  $\Lambda$  spin-flip M1 transition and the  $g$ -factor of the core nucleus ( $g_{\text{core}}$ ). The B(M1) of the  $\Lambda$  spin-flip M1 transition can be measured with Doppler shift attenuation method.

## 2. Hyperball and $\gamma$ spectroscopy of hypernuclei

Since the construction of the Hyperball in 1998,  $\gamma$  spectroscopy of hypernuclei has made a great progress. Five experiments were performed using the  $(\pi^+, K^+\gamma)$ ,  $(K^-, \pi^-\gamma)$ , and (stopped  $K^-$ ,  $\gamma$ ) reactions. In these experiments, germanium detectors were located around  $\pi^+$  or  $K^-$  beams available at KEK or BNL. Before the Hyperball was built, using germanium detectors with these meson beams was almost impossible.

In the previous  $\gamma$  ray measurements of hypernuclei,  $\Lambda N$  effective interactions and impurity effect were studied.

### 2.1. Hyperball

The Hyperball, which consists of 14 germanium detectors, covers 15 % of a solid angle for a point  $\gamma$ -ray source. The photo-peak efficiency of germanium detectors is about 2 for the  $\gamma$  ray at 1 MeV. Although there are serious background-induced problems in using germanium detectors for  $\gamma$  spectroscopy of hypernuclei, the Hyperball overcomes such difficulties with special readout electronics and BGO counters.

The BGO scintillation counters are used to suppress backgrounds from high energy  $\gamma$  rays from  $\pi^0$  mesons and Compton scattering. Modifications of readout electronics are also necessary to use germanium detectors under the condition of high intensity beam. When a high energy beam particle is scattered on the target and hits the germanium detectors, it gives an energy deposit of the order of 50 MeV. Since the energy deposit rate as well as the counting rate is extremely high, we need to use reset-type preamplifiers and fast shaping amplifiers with gated integrators.

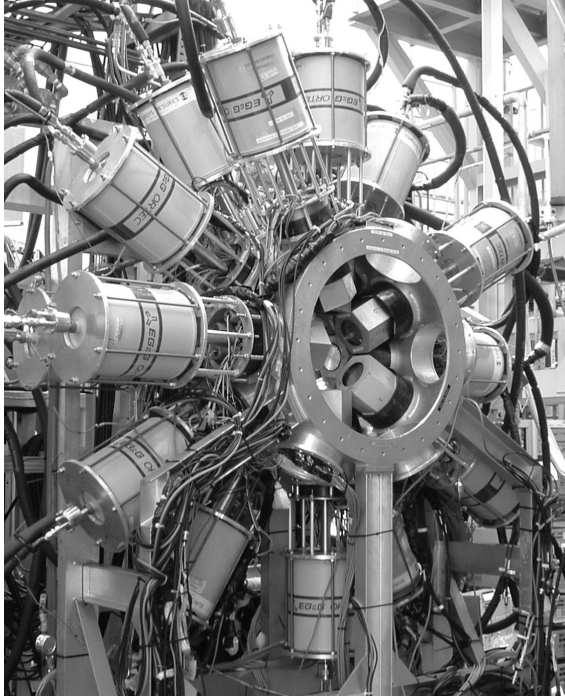


Fig. 2. Hyperball consists of 14 Ge detectors and BGO scintillation counters.

## 2.2. Present status of the experiments with the Hyperball

The first experiment with the Hyperball was performed at KEK-PS K6 beamline in 1998 (KEK-PS E419). Four  $\gamma$  transitions from  ${}^7_\Lambda\text{Li}$  including M1 ( $3/2^+ \rightarrow 1/2^+$ ) and E2 ( $5/2^+ \rightarrow 1/2^+$ ), were observed from the  ${}^7\text{Li}(\pi^+, K^+\gamma)$  reaction in this experiment. The spin-spin force and the nucleon induced spin-orbit force of  $\Lambda N$  effective interactions were investigated from these measured energy spacings [7]. The shrinkage of  ${}^7_\Lambda\text{Li}$  was also confirmed [4].

Using the  $(K^-, \pi^-\gamma)$  reaction, we carried out two experiments at BNL-AGS D6 beamline. In 1998,  $\gamma$  rays from  ${}^9_\Lambda\text{Be}$  were observed. The energy spacing of the  $\Lambda$  spin doublet ( $3/2^+, 5/2^+$ ) was measured and the  $\Lambda$ -spin-induced spin-orbit force was investigated [8]. Three years later, in order to determine the strength of the tensor force, we measured  $\gamma$  rays from  ${}^{16}_\Lambda\text{O}$  [9]. With this result, we completed to determine all the parameters for the spin-dependent terms of  $\Lambda N$  effective interactions. On the other hand, we also acquired the data with  ${}^{10}\text{B}$  target in this experiment, but did not observe  $\gamma$  rays from  ${}^{10}_\Lambda\text{B}$ . This result is inconsistent with the spin-dependent force parameters which were determined from the other hypernuclear data.

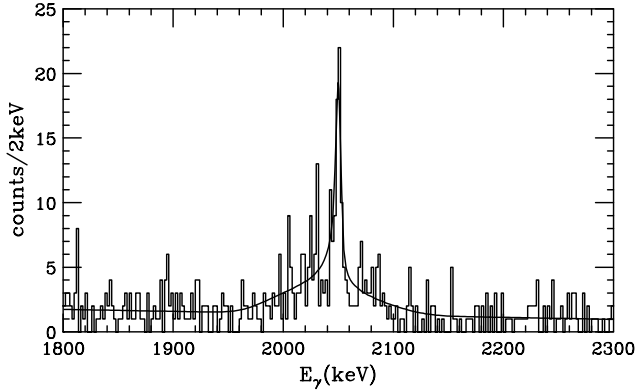


Fig. 3.  ${}^7_\Lambda\text{Li}$  ( $E2$ ;  $5/2^+ \rightarrow 1/2^+$ ): Result from KEK-PS E419 [4].  $B(E2)$  was measured from simulated peak shape (solid line) using Doppler shift attenuation method.

Although no  $\gamma$  rays were observed from  ${}^{10}_\Lambda\text{B}$ , we observed some  $\gamma$  transitions from hyperfragments with  ${}^{10}\text{B}$  target. Motivated by this result, we carried out an experiment to measure  $\gamma$  rays from hyperfragments using the stopped  $K^-$  method with several light targets ( ${}^7\text{Li}$ ,  ${}^9\text{Be}$ ,  ${}^{10}\text{B}$ ,  ${}^{11}\text{B}$ , and  ${}^{12}\text{C}$ ) at the KEK-PS K5 beamline [10]. From  ${}^{10}\text{B}$ ,  ${}^{11}\text{B}$ , and  ${}^{12}\text{C}$  targets, the  ${}^7_\Lambda\text{Li}$  ( $5/2^+ \rightarrow 1/2^+$ ) transition was observed again. Based on the measured production rate, the stopped  $K^-$  method seems to be a useful tool for  $\gamma$  spectroscopy of hypernuclei, particularly by using  $\gamma$ - $\gamma$  coincidence technique in the future.

### 3. A recent experiment — $\gamma$ spectroscopy of ${}^{11}_\Lambda\text{B}$

The latest experiment using the Hyperball (KEK-PS E518) was performed with the  ${}^{11}\text{B}(\pi^+, K^+\gamma)$  reaction at KEK in the autumn of 2002. The purpose of this experiment consists of two subjects.

The first subject is to investigate the spin dependent forces of  $\Lambda N$  effective interactions. Before this experiment, the strengths of the individual four terms have been already determined from experimental results with the Hyperball. However, cross check of these values using other hypernuclear data is still necessary.

Another subject is to measure the  $g$ -factor of  $\Lambda$  in a nucleus. At present,  ${}^{11}_\Lambda\text{B}$  ( $3/2^+ \rightarrow 1/2^+$ ) is considered to be the only  $\Lambda$ -spin-flip M1 transition in which we can measure the  $B(M1)$  with Doppler shift attenuation method within a reasonable beamtime.

3.1. Structure of  $^{11}_{\Lambda}B$

The structure of  $^{11}_{\Lambda}B$  is complicated. There are many bound states below the particle decay threshold into  $^{10}_{\Lambda}Be$  and a proton. Figure 4 shows the level scheme of  $^{11}_{\Lambda}B$  calculated by Millener [11]. In his calculation, excitation energies, branching ratios, and lifetimes of  $^{11}_{\Lambda}B$  bound states are estimated. Then, nine  $\gamma$  transitions are expected to be observed within a given beamtime.

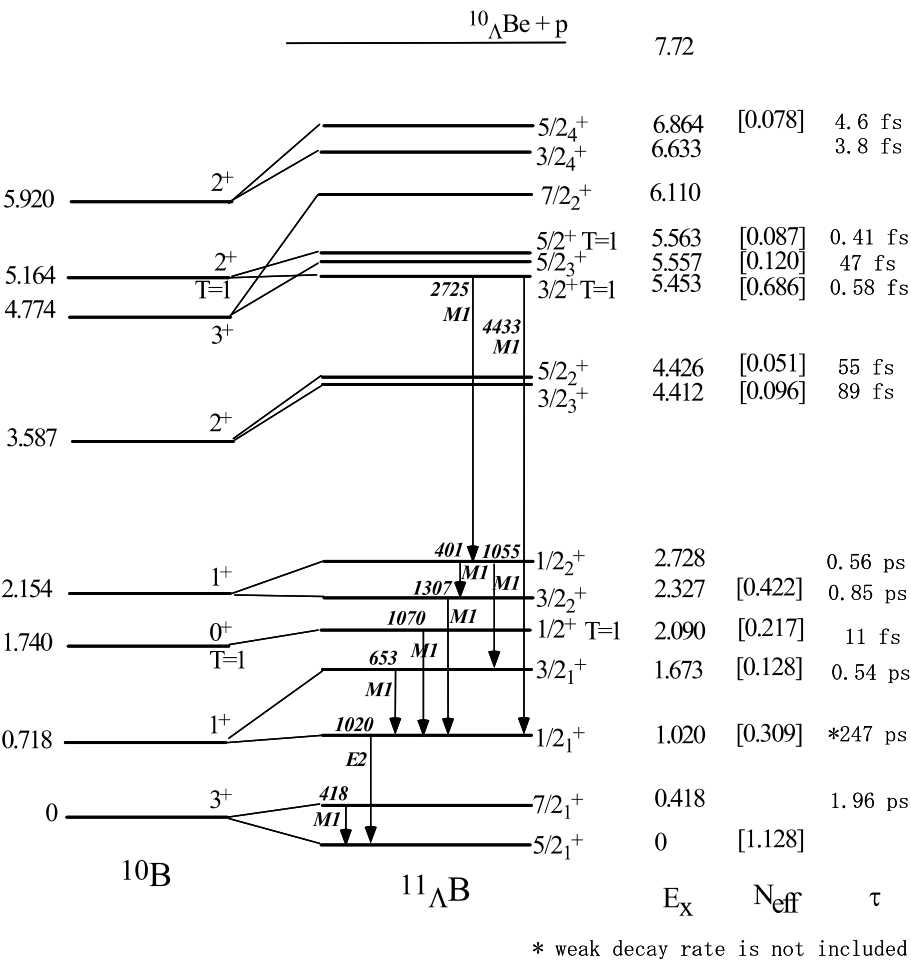


Fig. 4. Expected level scheme of  $^{11}_{\Lambda}B$  calculated by Millener [11]. Expected excitation energy, cross section, and lifetime of each state are listed on the right side. In total, nine  $\gamma$  transitions are expected to be observed in E518.

### 3.2. Experimental setup

Figure 5 shows the experimental setup of KEK-PS E518. The experiment was performed at the K6 beamline. At this beamline, high intensity  $\pi^+$  beam is available. The momentum of  $\pi^+$  was 1.04 GeV/c, and a typical beam intensity was  $4 \times 10^6$   $\pi^+$  per 1.2 second spill. In this experiment,  $^{11}\text{B}(\pi^+, K^+)$  reaction was used in producing  $^{11}_\Lambda\text{B}$ . Considering the  $\gamma$  ray yield, we used two kinds of thick targets whose thickness was 6 cm and 10 cm. The total amount of irradiation in one month was  $0.85 \times 10^{12} \pi^+$  for the 10 cm target and  $0.75 \times 10^{12} \pi^+$  for the 6 cm target.

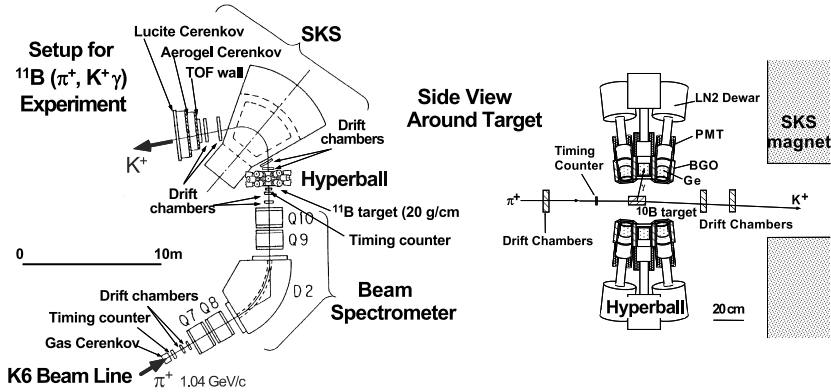


Fig. 5. Experimental setup of KEK-PS E518

The momenta of incident  $\pi^+$  and scattered  $K^+$  were measured with magnetic spectrometers. In particular, we used Superconducting Kaon Spectrometer (SKS) in measuring the momentum of the scattered  $K^+$ . This spectrometer was constructed to realize both high resolution and large acceptance [12]. The trajectory of each particle was reconstructed with drift chambers and used for calculation of the excitation energy and the momentum vector of the produced  $^{11}_\Lambda\text{B}$ . This information was used to choose the events in which bound states of  $^{11}_\Lambda\text{B}$  were produced, as well as to correct  $\gamma$ -ray energies for Doppler shift.

### 3.3. Results

From the analysis of the magnetic spectrometers, the excitation energy spectrum of  $^{11}_\Lambda\text{B}$  was obtained. In order to investigate the precise structure of this hypernucleus, a measurement with a thin ( $2 \text{ g/cm}^2$ ) target was also performed. The thin-target spectrum is shown in Fig. 6 (top). The horizontal axis of this spectrum has the scale of the binding energy of  $\Lambda$  ( $-B_\Lambda$ ) defined as

$$-B_\Lambda = M_{\text{hyp}} - M_\Lambda - M_{\text{core}}. \quad (3)$$



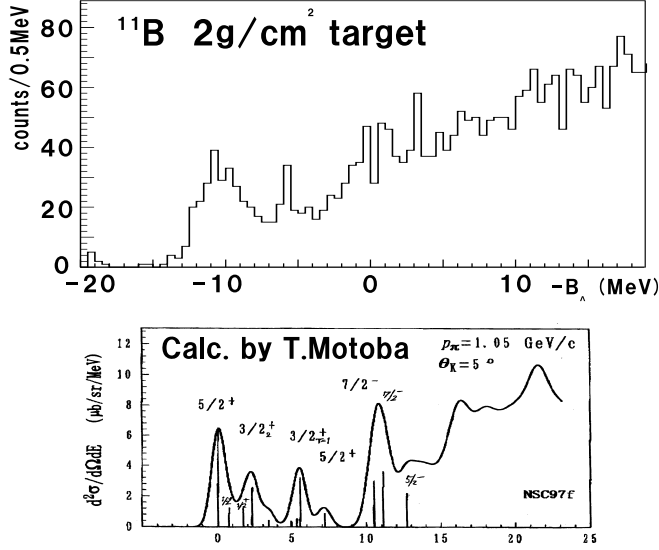


Fig. 6. Exciting energy spectra of  $^{11}\text{B}$ . Upper spectrum is measured with a thin target. Lower spectrum is the theoretically calculated one by Motoba [13].

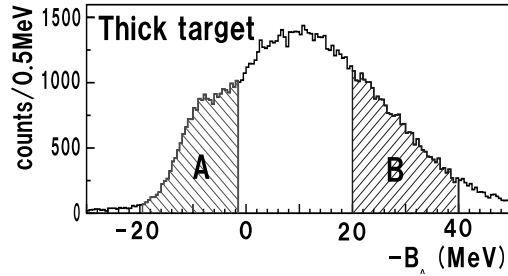


Fig. 7. Excitation energy spectrum with the thick targets. The region A is selected for bound states, and B is selected for highly unbound states.

Here,  $M_{\text{hyp}}$  is the mass of the hypernucleus,  $M_A$  is the mass of  $A$ , and  $M_{\text{core}}$  is the mass of the core nucleus. Comparing this spectrum with a theoretical calculation by Motoba [13], which is shown in the lower spectrum of Fig. 6, we can see that the spectra resemble each other.

Figure 7 shows the mass spectrum obtained with the thick targets. In this mass spectrum, the energy resolution is worse than that with the thin target. To observe  $\gamma$  rays, the region "A" ( $-20 \text{ MeV} < -B_A < -2 \text{ MeV}$ ) is selected as the bound state region, and the region "B" ( $20 \text{ MeV} < -B_A < 40 \text{ MeV}$ ) is selected as the highly unbound region.

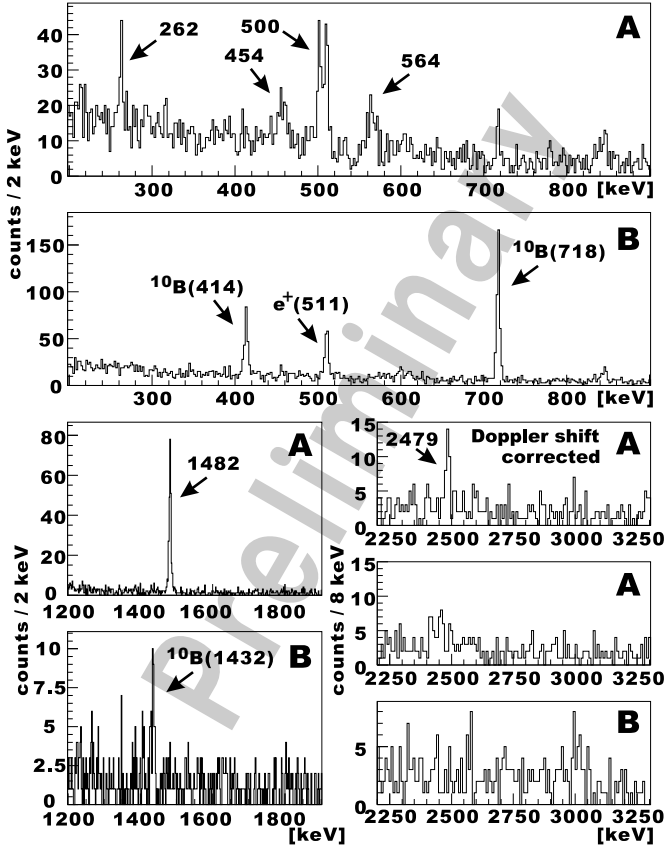


Fig. 8.  $\gamma$  ray spectra for  $^{11}\text{B}$ . By comparing spectra for two regions, namely A ( $-20 \text{ MeV} < -B_A < -2 \text{ MeV}$ ) and B ( $20 \text{ MeV} < -B_A < 40 \text{ MeV}$ ), six  $\gamma$  transitions from  $^{11}\text{B}$  are observed. The 2478 keV peak is observed after Doppler shift correction.

Figure 8 shows preliminary results of the observed  $\gamma$  ray spectra from these regions. By comparing the  $\gamma$  ray spectra for the A and B regions, six  $\gamma$  ray peaks at 262 keV, 454 keV, 500 keV, 564 keV, 1482 keV, and 2479 keV are identified as the  $\gamma$  transitions in  $^{11}\text{B}$ , because they are observed only in the bound state region. Among these  $\gamma$  rays, the 2479 keV peak is observed after Doppler shift correction. The observed number of events and the relative intensity for each  $\gamma$  transition are listed in Table I. In the relative intensity, energy dependence of the germanium detector efficiency is taken into account, and then it is normalized with the number of events for the 1482 keV  $\gamma$  ray.

TABLE I

Number of events and relative intensities for observed  $\gamma$  transitions. Relative intensities are normalized by the number of events for the 1482 keV  $\gamma$  ray.

$E_\gamma$ (keV)	Number of event	Relative intensity
262	68	0.09
454	49	0.10
500	77	0.16
564	61	0.17
1482	225	1.00
2479	20	0.13

### 3.4. Identification of observed $\gamma$ rays

Identification of the observed  $\gamma$  transitions is not easy because there are many possible candidates for level assignment. However, the 1482 keV  $\gamma$  transition can be identified from the following three points.

At first, estimated from the peak width, this  $\gamma$  ray peak is not broadened by Doppler effect. Therefore, the lifetime of this transition should be longer than 10 psec. If this transition is M1,  $B(M1)$  is smaller than  $10^{-3}\mu_N^2$ . As it is too small, this  $\gamma$  ray should be identified as E2.

Next, this  $\gamma$  transition has the largest yield. According to the Millener's prediction [11], the E2 ( $1/2^+ \rightarrow 5/2^+$ ) transition is expected to have the largest yield.

In addition, from the excitation energy spectrum of  $^{11}\text{B}$  plotted by choosing those events which have  $\gamma$  rays at 1482 keV, we found that this  $\gamma$  ray is emitted not only from the region near the ground state, but also from the higher excited bound states. This situation is consistent with the property of the E2 ( $1/2^+ \rightarrow 5/2^+$ ) transition that the  $5/2^+$  state is populated not only directly by the reaction but through higher excited states by  $\gamma$  ray cascade.

Therefore, this 1482 keV  $\gamma$  ray is identified as  $^{11}\text{B}$  ( $1/2^+ \rightarrow 5/2^+$ ) transition. To identify other transitions,  $\gamma$ - $\gamma$  coincidence is necessary. Due to low statistics, however, this method seems almost impossible. We need more beam time to identify all the observed transitions.

### 3.5. Comparison with theory

Using the results of the previous experiments, the effective interaction parameters are determined as follows:

$$\begin{aligned}\Delta &= 0.5 \text{ MeV [10]}, \quad S_N = -0.4 \text{ MeV [10]}, \\ S_A &= -0.01 \text{ MeV [8]}, \quad T = 0.03 \text{ MeV [9]}.\end{aligned}\tag{4}$$

For the identified E2 transition of  ${}_{\Lambda}^{11}\text{B}$ , the energy is given by the following equation from a shell model calculation by Millener [11].

$$\begin{aligned} \Delta E \left( \frac{1}{2}_1^+ \rightarrow \frac{5}{2}_1^+ \right) &= 0.243\Delta - 1.090S_N + 1.234S_A - 1.627T + \Lambda\Sigma + 718 \text{ keV} \\ &= 1020 \text{ keV} \end{aligned} \quad (5)$$

Here,  $\Lambda\Sigma$  means the three-body force effect which is related to two-pion exchange with a  $\Sigma$  in intermediate state. The three-body force is calculated in the case of  $s$ -shell hypernuclei by Akaishi *et al.* [15], and applied to  $p$ -shell by Millener [3]. If we substitute spin-dependent parameters in Eq. (5) by Eq. (4), this energy becomes 1020 keV.

In Table II, the measured and expected energies are compared for the transitions observed in previous experiments. The energy spacings shown in the first four lines of this table are used to determine the spin-dependent parameters of  $\Lambda N$  interaction shown in the last column. For the next three transition, the expected energy seems consistent with the measured one within 100 keV. In case of  ${}_{\Lambda}^{11}\text{B}$  ( $E2; 1/2^+ \rightarrow 5/2^+$ ), however the difference is more than 400 keV.

TABLE II

Comparison of measured and expected energy spacings of  $p$ -shell hypernuclei (see text). The last column shows the spin-dependent force parameter which has the largest contribution to the energy spacing.

Levels	Measured energy spacing	Expected energy spacing	Spin-dependent term
${}_{\Lambda}^7\text{Li} (3/2^+, 1/2^+)$	692 keV [4]		$\Delta$
${}_{\Lambda}^7\text{Li} (5/2^+, 1/2^+)$	2050 keV [4]		$S_N$
${}_{\Lambda}^9\text{Be} (3/2^+, 5/2^+)$	48 keV [8]		$S_A$
${}_{\Lambda}^{16}\text{O} (0^-, 1_1^-)$	26 keV [9]		$T$
${}_{\Lambda}^7\text{Li} (1/2_2^+, 1/2_1^+)$	3877 keV [4]	3779 keV [11]	$S_N$
${}_{\Lambda}^{13}\text{C} (3/2^+, 1/2^+)$	4880 keV [14]	4831 keV [11]	$S_N$
${}_{\Lambda}^{16}\text{O} (1_2^-, 1_1^-)$	6534 keV [9]	6435 keV [11]	$S_N$
${}_{\Lambda}^{11}\text{B} (1/2_1^+, 5/2_1^+)$	1482 keV	1020 keV [11]	$S_N$

The energies for the last four transitions in Table II are mainly determined by  $S_N$ . If we determine  $S_N$  from the measured E2 energy of  ${}_{\Lambda}^{11}\text{B}$ , this parameter becomes  $-0.9$  MeV. It is much different from the value of  $-0.4$  MeV obtained from  ${}_{\Lambda}^7\text{Li}$ . From the other transitions,  $-0.9$  MeV is also unacceptable. Therefore, only  ${}_{\Lambda}^{11}\text{B}$  seems inconsistent with other results. It suggests that the present experimental data are not enough to confirm  $\Lambda N$  spin-dependent interaction.

#### 4. Summary

An experiment for  $\gamma$  spectroscopy of  ${}^{11}_{\Lambda}\text{B}$  (KEK-PS E518) was performed to confirm  $\Lambda N$  effective interaction parameters and to measure the magnetic moment of  $\Lambda$  in a nucleus.

Using the  $(\pi^+, K^+)$  reaction, six  $\gamma$  transitions from  ${}^{11}_{\Lambda}\text{B}$  were observed. Among the observed  $\gamma$  transitions, the 1482 keV  $\gamma$  ray was identified as  ${}^{11}_{\Lambda}\text{B}$  ( $E2; 1/2^+ \rightarrow 5/2^+$ ), but its energy is different from a theoretical prediction. It seems interesting to investigate structure of several more hypernuclei to confirm  $\Lambda N$  interaction.

In order to identify all of the  $\gamma$  transitions observed in this experiment,  $\gamma$ - $\gamma$  coincidence method is necessary. Due to low statistics, it is difficult to identify them with the present data, but it will be possible in near future by using an upgraded Hyperball.

#### REFERENCES

- [1] R.H. Dalitz, A. Gal, *Ann. Phys.* (N.Y.) **116**, 167 (1978).
- [2] D.J. Millener, A. Gal, C.B. Dover, R.H. Dalitz, *Phys. Rev.* **C31**, 499 (1985).
- [3] D.J. Millener, *Nucl. Phys.* **A691**, 93c (2001).
- [4] K. Tanida *et al.*, *Phys. Rev. Lett.* **86**, 1982 (2001).
- [5] T. Motoba, H. Bandō, K. Ikeda, *Prog. Theor. Phys.* **80**, 189 (1983).
- [6] E. Hiyama, M. Kaminuma, K. Miyazaki, T. Motoba, *Phys. Rev. Lett.* **86**, 1982 (2001).
- [7] H. Tamura *et al.*, *Phys. Rev. Lett.* **84**, 5963 (2000).
- [8] H. Akikawa *et al.*, *Phys. Rev. Lett.* **88**, 082501 (2002).
- [9] H. Tamura *et al.*, *Proc. Int. Symp. on Electrophoto-production of Strangeness on Nucleons and Nuclei (SENDAI03)*, June 2003, World Scientific, Ed. K. Maeda *et al.*, to be published.
- [10] K. Tanida *et al.*, *Nucl. Phys.* **A721**, 999c (2003).
- [11] D.J. Millener, private communication.
- [12] T. Fukuda *et al.*, *Nucl. Instrum. Methods* **A361**, 485 (1995).
- [13] T. Motoba, private communication.
- [14] H. Kohri *et al.*, *Phys. Rev.* **C65**, 034607 (2002).
- [15] Y. Akaishi, T. Harada, S. Shinmura, K.S. Myint, *Phys. Rev. Lett.* **84**, 3539 (2000).